

Design and Characterization of a Novel Hybrid-field Ion-Guide as part of a TOF MS Platform

Alexander Lekkas; Athanasios Zacharos; Diamantis Kounadis; Ioannis Orfanopoulos; Dimitris Papanastasiou; Emmanuel Raptakis
Fasmatech Science & Technology, Athens, GR

INTRODUCTION

A novel design of a Radio-Frequency (RF) octapole ion guide arrangement forming multiple longitudinal segments is described using gas dynamics calculations and ion optics simulations. The ion guide is constructed and further evaluated experimentally on a prototype orthogonal Time-of-Flight Mass Spectrometry (TOF MS) platform. The octapole is structurally configured to produce multipolar RF field distributions of different order throughout the geometry. The octapolar field is formed at the entrance to enhance acceptance, which is particularly useful for capturing ions entrained in diffusive jet flows emerging from narrow pressure limiting apertures, while the quadrupolar field established toward the exit compresses radial phase and confines the ion beam on axis. Investigations using ion optical simulations incorporating realistic low pressure gas flows provide insights to help interpret experimental results and improve design and performance.

THEORY

The underlying concept of the RF ion guide design is the formation of lower order electric field distributions derived from higher order multipole geometrical arrangements. The potential distribution of a multipole geometry is computed by the following expression [1]:

$$\Phi(r, \varphi) = \Phi_o \left(\frac{r}{r_o} \right)^n \cos n\varphi$$

where n is the order of the multipole field distribution ($n=2$ for quadrupole, $n=4$ for octapole), $2n$ is the number of electrodes or poles, φ is the angle of the electrode, and Φ_o , r_o are the maximum potential and inscribed radius of the multipole respectively. The voltage applied on each of the poles of a multipole arrangement is determined by setting $r=r_o$ and the expression can be reduced to $V = V_o \cos n\varphi$, where V is the voltage on each pole and V_o the maximum amplitude. The expression used for approximating the pseudopotential well produced from a lower field-order using a higher order multipole configuration is [1]:

$$V^* = \frac{n^2 e V^2}{4 m \Omega^2 r_o^2} \left(\frac{r}{r_o} \right)^{2n-2}$$

where e is the electron charge, m the ion mass, V is the 0-p RF voltage and Ω is the RF angular frequency. A significant practical consideration deduced from the equation is the increasing depth of the effective potential with field-order to efficiently confine ions with extended kinetic energy and positional spreads. In contrast, lower field-order distributions appear suitable for focusing ions to improve transmission through narrow apertures.

DIRECT SIMULATION MONTE CARLO

Computations to solve for the diffusive jet emerging from the end-aperture of an ion funnel operated at 5 mbar and discharging inside the octapole ion guide at 10^{-2} mbar are performed using the Direct Simulation Monte Carlo (DSMC) method. A 3D model of the ion guide is constructed in SALOME™ and the flow field is computed in OpenFOAM™. Inlet boundary conditions are obtained by solving the entire flow field inside the ion funnel [2]. The octapole geometry consists of eight 20 mm long electrodes equally spaced (1mm) in the axial direction. The inscribed radius is 4 mm and the 10^{-2} mbar pressure boundary is defined at 7.5 mm from the axis.

The 45° slice shown in Figure 1 (a) is used to generate the 180 mm long 3D mesh and contains a single electrode centered at 0°. The mesh in the near-field region of the diffusive jet is “unstructured” to satisfy cell size requirements while a “structured” mesh is used throughout the remaining volume with a total number of ~7.5 M cells. Figures 1 (b) and (c) show axial (X) and radial (Z) velocity components respectively for nitrogen gas discharging from a 1.6 mm aperture into the 10^{-2} mbar pressure region. A diffusive jet with strong axial (>600 m/s) and radial (> 400 m/s) velocity components develops throughout the length of the first segment (20 mm). The penetration depth is significantly shorter compared to the supersonic jet formed in the fore vacuum region, however, expansion in the radial dimension appears substantially enhanced. Figure 1 (c) shows 3D axial velocity contours in steps of 50 m/s. The gas expands radially through the gap between electrodes.

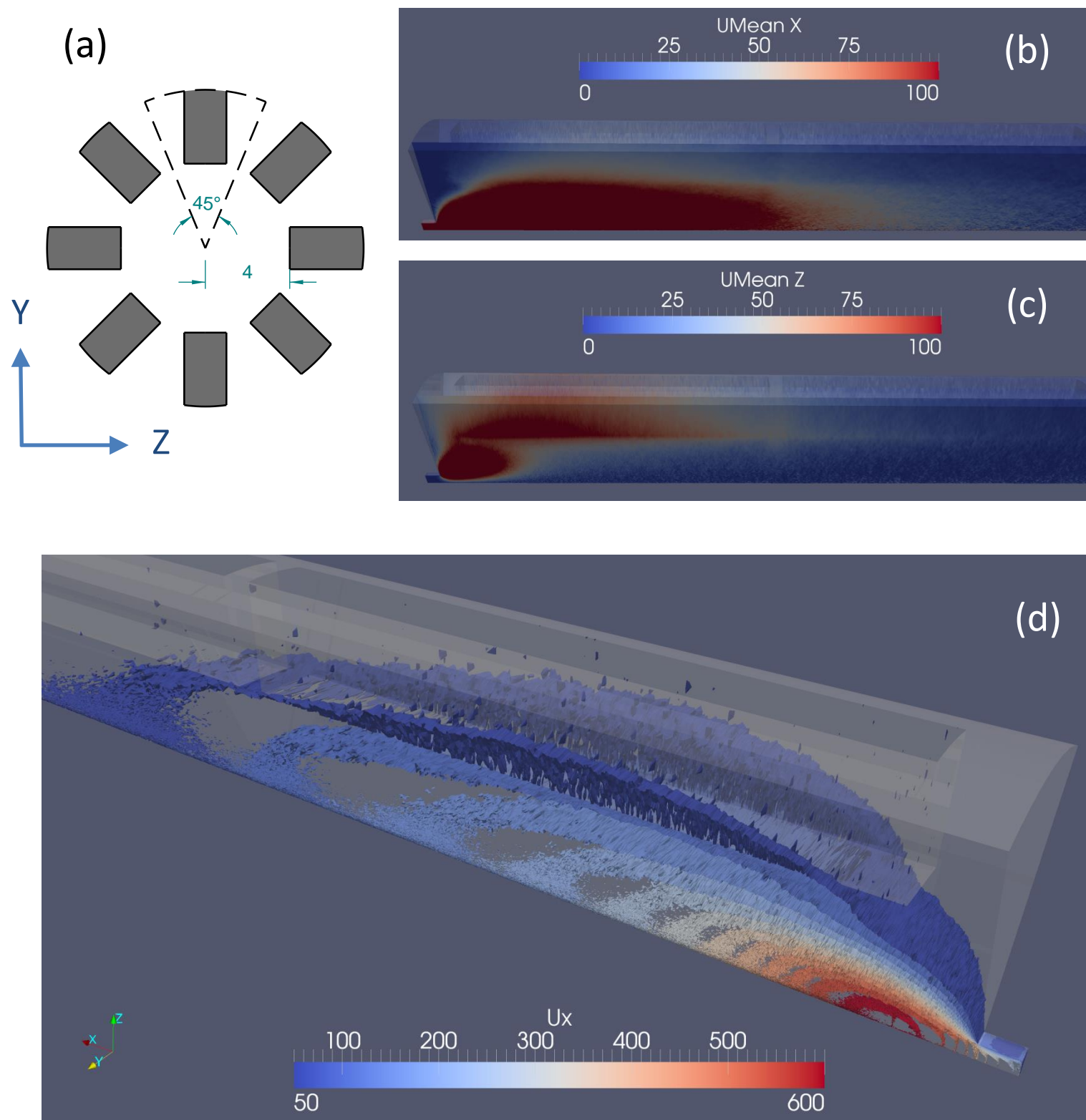


FIGURE 1. (a) Octapole cross section highlighting 45° slice for DSMC calculations, (b) axial and (c) radial velocity components across the first segment and (d) 3D contours of the axial velocity in steps of 50 m/s.

ION OPTICS SIMULATIONS

Post-processing of the DSMC solution for the flow field was performed and introduced in SIMION. Ion tracing was carried out using hard sphere collisions. Transmission of ions with m/z values corresponding to cesium and cesium-iodide cluster ions was carried out for (a) a combination of octapolar and quadrupolar fields at the entrance and exit of the ion guide respectively and (b) a pure quadrupolar field established throughout the device. Simulation results with and without the DSMC flow field are also presented to demonstrate the effect of the diffusive jet.

Figure 2 shows ion trajectories for $\text{Cs}_{n+1}\text{I}_n^+$ ions ($n=0,1..8$) injected into the octapole in the presence of the low-pressure diffusive jet. Significant ion losses are observed for the quadrupolar field distribution, shown in Figure 2 (b) where ions are lost on the electrodes of the first segment. In contrast transmission efficiency for the octapolar field is superior, as shown in Figure 2 (a). In the latter case phase space compression is observed over the last three segments where the field-order applied is quadrupolar. The amplitude of the voltage waveform applied to the octapolar field of the ion guide is 50 V_{0-p} and 150 V_{0-p} for the quadrupolar field, while frequency is fixed at 1.5 MHz.

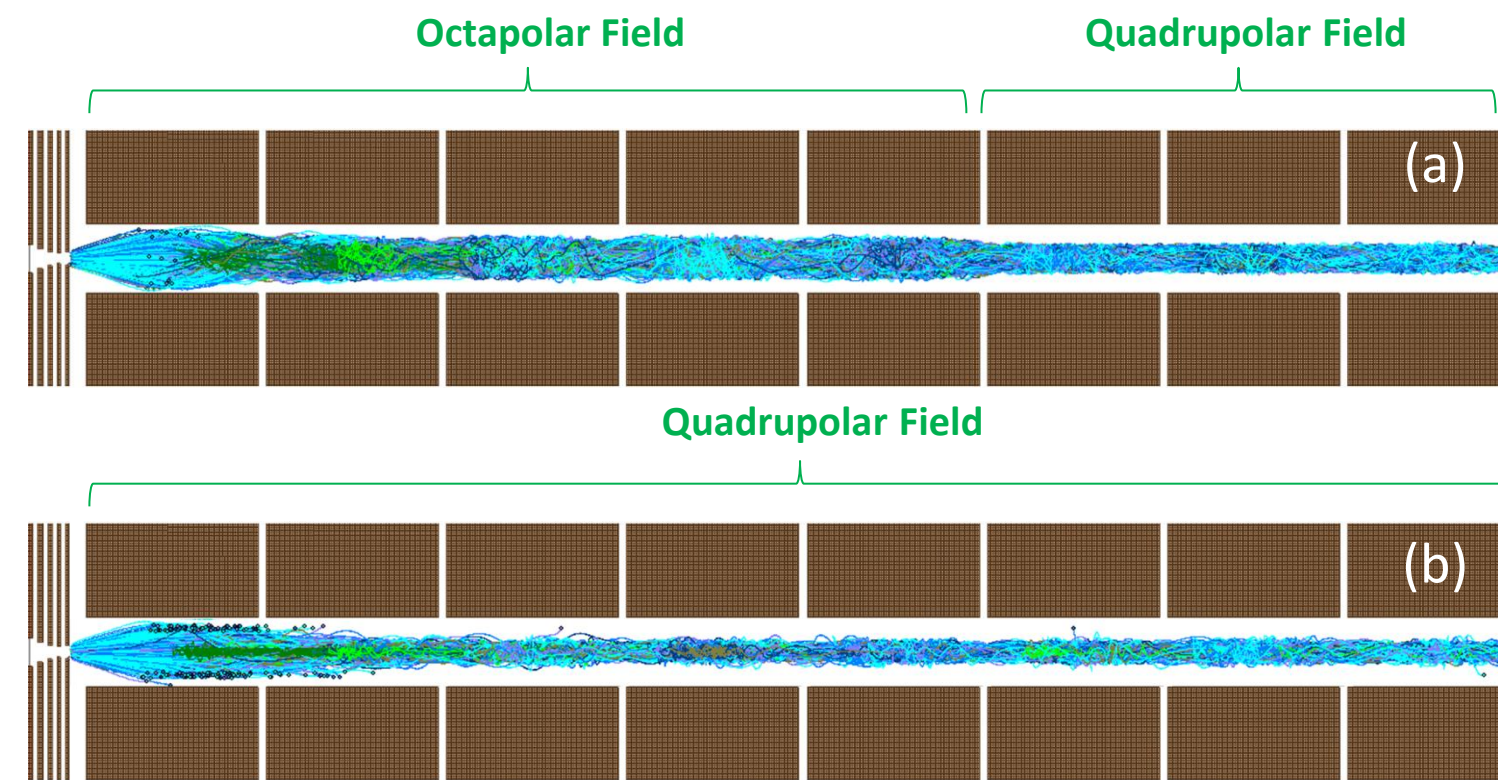


FIGURE 2. Ion trajectories for m/z values corresponding to cesium-iodide ions over a wide mass range extending from $m/z=133$ to $m/z=1952$. (a) Ion guide combining octapolar and quadrupolar fields and (b) ion guide with quadrupolar field only.

Figure 3 (a) shows simulated transmission efficiency for the two operating modes of the ion guide as discussed with reference to Figure 2, with and without the DSMC flow field. The low transmission efficiency observed for the quadrupolar field is partly attributed to the narrow phase space acceptance at the entrance of the ion guide. The effect of the gas flow field is pronounced and affects the entire mass range. For the quadrupolar field the corresponding q value is also shown across the mass range. The octapolar field exhibits superior transmission extending from the low-mass cut off of the device across the entire mass range investigated. The effect of the flow becomes apparent for $m/z>1500$ where the effective potential well grows shallow. Figure 3 (b) shows transmission efficiency for Cs_8I_7^+ , 1952 amu and for the two operating modes as a function of waveform amplitude. The frequency of the trapping waveform is 1.5 MHz.

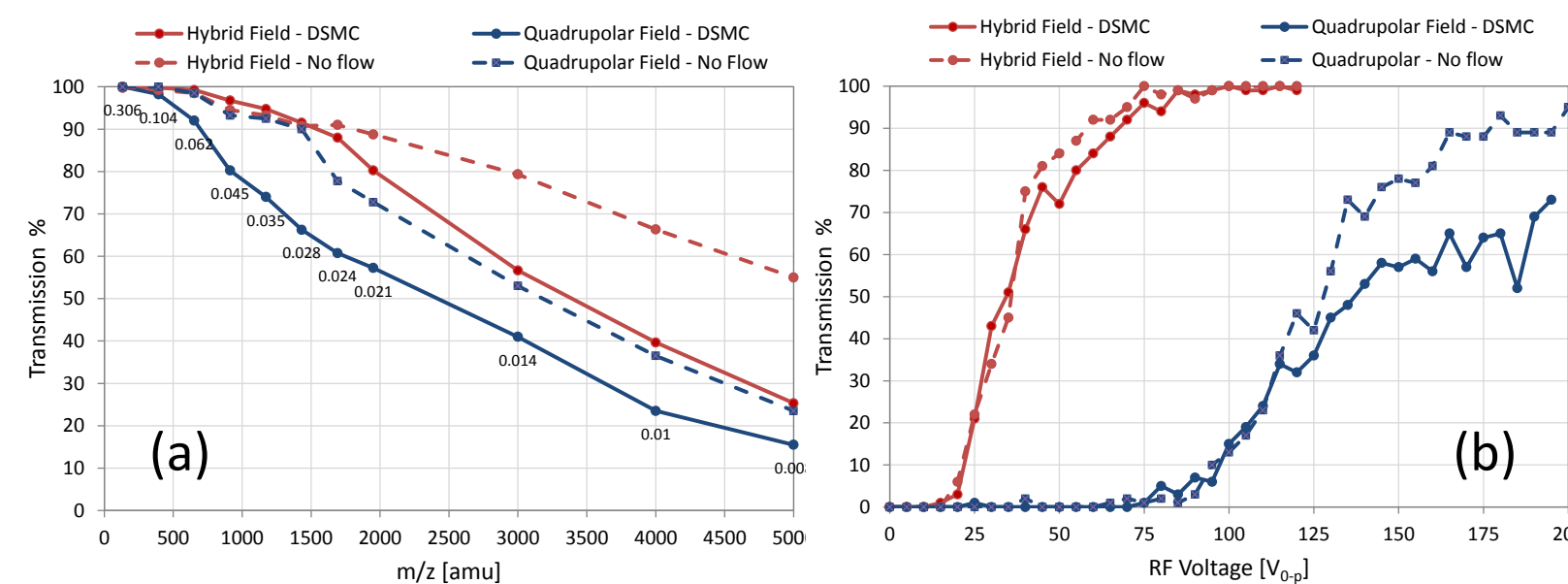


FIGURE 3. (a) Simulated transmission efficiency across a wide mass range for the two modes of operation discussed with reference to Figure 2 and (b) transmission efficiency for Cs_8I_7^+ ion as a function of waveform amplitude.

EXPERIMENTAL RESULTS

A 3D CAD model and the assembled octapole ion guide are shown in Figures 4 (a) and 4 (b) respectively. A pair of insulating rings (PEEK) radially slotted to position the electrodes of each segment are matched together using high tolerance machining. Each pair carrying eight electrodes and forming a single segment are then compressed together using a PEEK flange at the entrance and a stainless steel ring at opposite ends. The PEEK flange is also used for positioning the DC lens electrodes at the entrance of the ion guide. A PCB RC network mounted on top of the ion guide assembly runs across its entire length to deliver the RF and DC signals. Signal distribution to all electrodes is achieved via phosphor bronze spring-connectors. The ion guide is installed in the second vacuum region of a prototype orthogonal TOF MS, shown in Figure 4 (c).

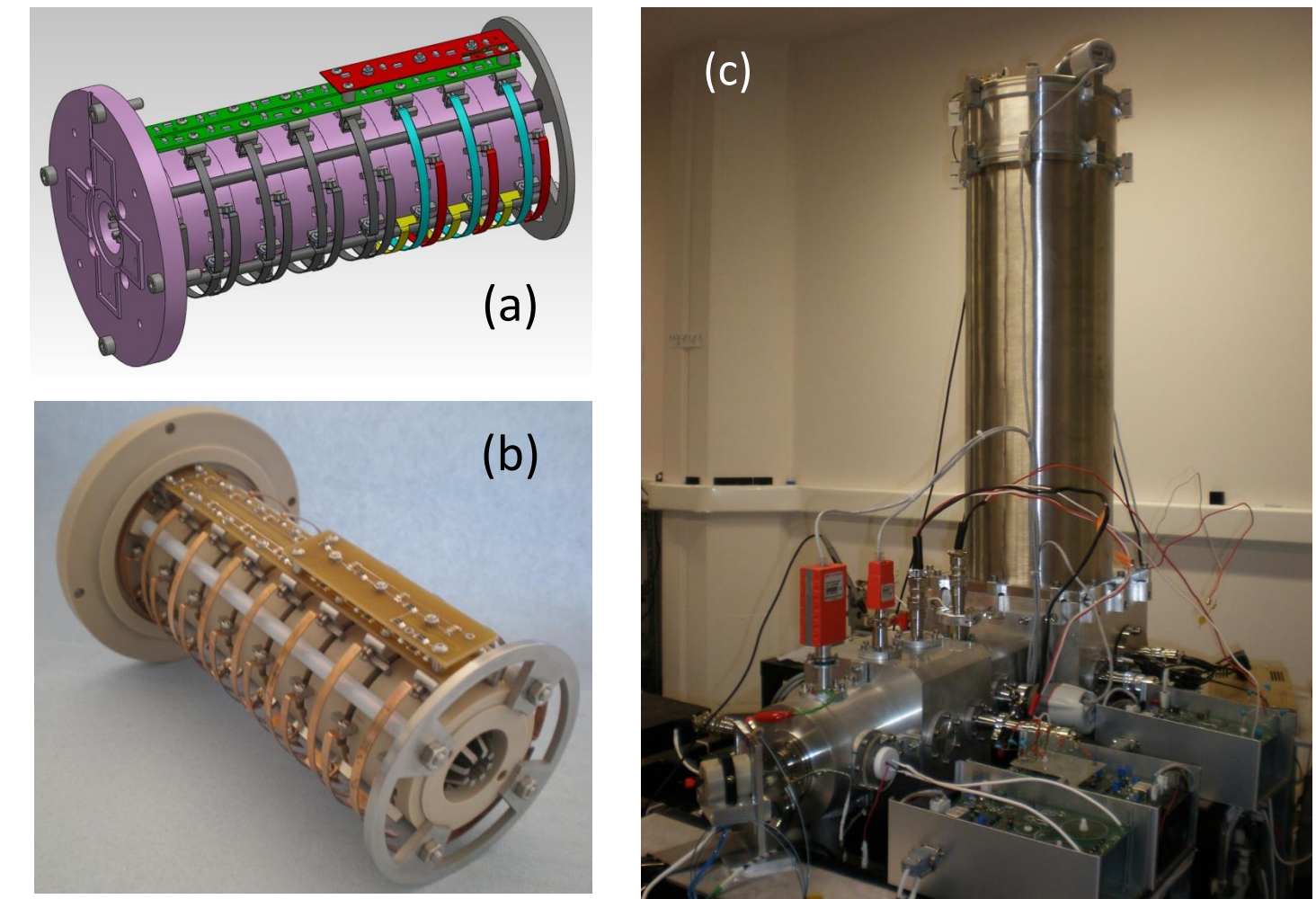


FIGURE 4. (a) 3D CAD model and (b) assembly of the segmented octapole ion guide. (c) prototype oTOF MS system incorporating the ion guide.

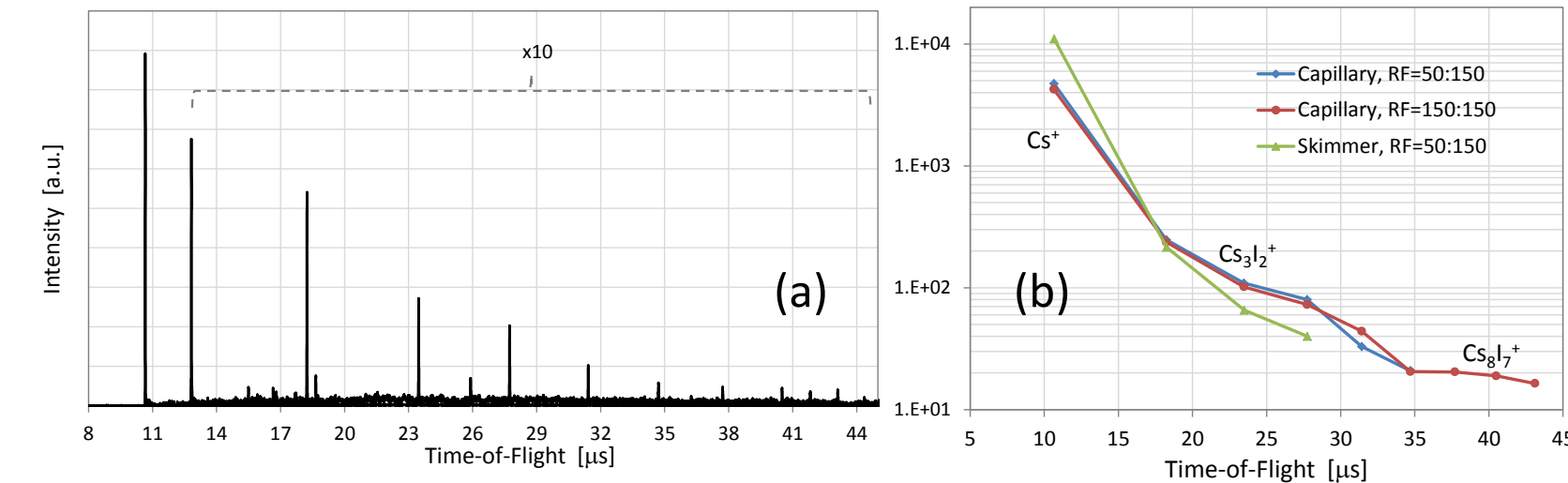


FIGURE 5. (a) TOF spectrum of cesium-iodide and (b) transmission efficiency across the mass range for different ion guide settings.

Cesium-iodide was infused at 2 $\mu\text{L}/\text{min}$ using ESI. The Cs^+ ion dominates the mass spectrum shown in Figure 5 (a). Figure 5 (b) shows experimental transmission efficiency obtained with a skimmer inlet aperture and a capillary inlet. Results show the effect of varying the ratio of the RF waveform voltage amplitude of the octapolar and quadrupolar fields.

REFERENCES

- [1] D. Gerlich. Inhomogeneous RF fields: A versatile tool for the study of processes with slow ions. Adv. Chem. Phys., 82 (1992), p. 1
- [2] Zacharos A. *et al*, ThP 079, 61st ASMS Conference on Mass Spectrometry and Allied Topics, June 9 - 13, 2013 Minneapolis, MN

